

# Local chemical transformations in poly(dimethylsiloxane) by irradiation with 248 and 266 nm

Vera-Maria Graubner<sup>a</sup>, Oskar Nuyken<sup>a</sup>, Thomas Lippert<sup>b,\*</sup>,  
Alexander Wokaun<sup>b</sup>, Sylvain Lazare<sup>c</sup>, Laurent Servant<sup>c</sup>

<sup>a</sup> Technische Universität München, Lehrstuhl für Makromolekulare Stoffe, Lichtenbergstr. 4, 85747 München, Germany

<sup>b</sup> Paul Scherrer Institut, General Energy Research Department, 5232 Villigen PSI, Switzerland

<sup>c</sup> Université de Bordeaux I, Laboratoire de Physico-Chimie Moléculaire, 33405 Talence Cedex, France

Received 3 May 2005; accepted 18 July 2005

Available online 27 October 2005

## Abstract

Poly(dimethylsiloxane) (PDMS) has been irradiated with a frequency quadrupled Nd:YAG laser and a KrF<sup>\*</sup>-excimer laser at a repetition rate of 1 Hz. The analysis of ablation depth versus pulse number data reveals a pronounced incubation behavior. The thresholds of ablation (266 nm: 210 mJ cm<sup>-2</sup>, 248 nm: 940 mJ cm<sup>-2</sup>) and the corresponding effective absorption coefficients  $\alpha_{\text{eff}}$  (266 nm: 48900 cm<sup>-1</sup>, 248 nm: 32700 cm<sup>-1</sup>,  $\alpha_{\text{lin}} = 2 \text{ cm}^{-1}$ ) were determined. The significant differences in the ablation thresholds for both irradiation wavelengths are probably due to the different pulse lengths of both lasers. Since the shorter pulse length yields a lower ablation threshold, the observed incubation can be due to a thermally induced and/or a multi-photon absorption processes of the material or impurities in the polymer.

Incubation of polymers is normally related to changes of the chemical structure of the polymer. In the case of PDMS, incubation is associated with local chemical transformations up to several hundred micrometers below the polymer surface. It is possible to study these local chemical transformations by confocal Raman microscopy, because PDMS is transparent in the visible. The domains of transformation consist of carbon and silicon, as indicated by the appearance of the carbon D- and G-bands between 1310 and 1610 cm<sup>-1</sup>, a band appearing between 502 and 520 cm<sup>-1</sup> can be assigned to mono- and/or polycrystalline silicon.

The ablation products, which are detected in the surroundings of the ablation crater consist of carbon and amorphous SiO<sub>x</sub> ( $x \approx 1.5$ ) as detected by infrared spectroscopy.

© 2005 Elsevier B.V. All rights reserved.

**Keywords:** Poly(dimethylsiloxane) (PDMS); Irradiation and laser ablation; Chemical transformation

## 1. Introduction

Poly(dimethylsiloxane) (PDMS) is an important technical polymer, and the modification of the surface is a growing research field. One possible approach for modifying the surface is the application of UV irradiation. Surface modification can result in the conversion of the polymer surface from hydrophobic to hydrophilic without etching or physical structuring. The surface modification of poly(dimethylsiloxane) by ultraviolet radiation in the presence of atmospheric oxygen [1–5] or by plasmas generated by partial corona discharge [6–12] has been reported previously. However, these

techniques do not allow a structuring or lateral resolved modification of the surface without using a mask. In spite of the low linear absorption coefficient ( $\approx 2 \text{ cm}^{-1}$ ) of poly(dimethylsiloxane) (Fig. 1) at 248 and 266 nm, it is possible to structure PDMS with lasers emitting at these wavelengths applying fluences  $< 1 \text{ J cm}^{-2}$ . This behavior is possible, because incubation occurs which changes the material and increases the absorption coefficient [13,14]. Incubation can occur up to a few micrometers below the surface by chemical modification or, as in our experiments, by local chemical transformations up to several hundred micrometers below the polymer surface, which causes an increase of the absorption at the appropriate wavelength.

This paper presents data obtained by analyzing the local chemical transformations with confocal Raman microscopes and the ablation products with infrared spectroscopy on cross-

\* Corresponding author. Tel.: +41 56 310 4076; fax: +41 56 310 2485.

E-mail address: [Thomas.Lippert@psi.ch](mailto:Thomas.Lippert@psi.ch) (T. Lippert).

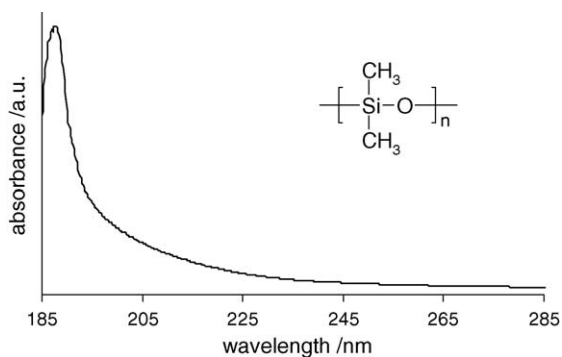


Fig. 1. UV absorption spectra of PDMS.

linked PDMS surfaces after irradiation with a KrF<sup>\*</sup>-excimer laser (248 nm) and a frequency quadrupled Nd:YAG laser (266 nm). Since PDMS is an optical transparent polymer it is possible to examine the chemical transformations below the surface.

## 2. Experimental

Films of cross-linked poly(dimethylsiloxane) (PDMS) have been prepared by evaporating a 12 wt% solution of vinyl-functionalized poly(dimethylsiloxane), poly(methylsiloxane) as a cross-linker and a Kartstedt platinum catalyst in isooctane in polystyrene Petri dishes. The films are cured for 5 min at 100 °C after evaporation of the solvent. The resulting film thickness (average of about 400 μm) was measured by a profilometer (Dektak 8000).

As irradiation sources, a frequency quadrupled ( $\lambda = 266$  nm) Nd:YAG laser (Quantel Brilliant B, 1 Hz,  $\tau = 6$  ns) and a KrF<sup>\*</sup>-excimer laser (Lambda Physik (Göttingen) LPX 220i, 1 Hz,  $\tau = 25$  ns) were used. The laser beam was focused with a spherical lens onto the sample surface after passing an attenuator and a homogenizer (only for 248 nm). The etch depth of the irradiated area was determined by a profilometer (266 nm) and by optical focusing with the confocal Raman microscope (248 nm) on the surface and at the bottom of the craters.

Raman spectra were measured after irradiation with the Nd:YAG laser (266 nm) with a Raman microscope (Labram, DILOR) equipped with an objective (50× magnification) and a thermoelectrically cooled charge-coupled detector and a HeNe laser as excitation source. The spectral resolution was 4 cm<sup>-1</sup>.

After irradiation with the KrF<sup>\*</sup>-excimer laser Raman spectra were recorded with a confocal Raman microscope (Labram, IMAGE) equipped with an objective (50× magnification) and an argon ion laser operating at 514.5 nm (spectral resolution 4 cm<sup>-1</sup>).

ATR-FTIR spectra were recorded with a Nicolet Magna-IR 560 spectrometer equipped with a Spectra-Tech ATR-objective (15× and 25× magnification, ZnSe) and a nitrogen cooled MTC detector with spectral resolution of 4 cm<sup>-1</sup>.

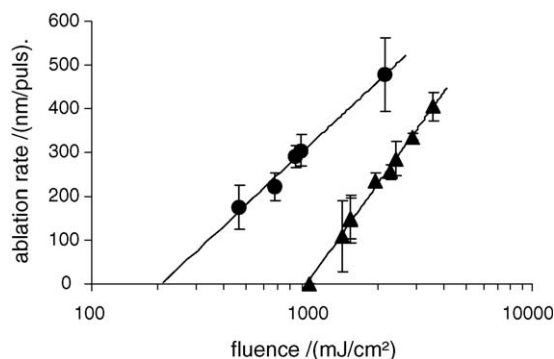


Fig. 2. Plot of etch depth per pulse vs. fluence: (▲) 248 nm and (●) 266 nm.

## 3. Results and discussion

### 3.1. Ablation threshold and effective absorption coefficient

PDMS was irradiated with a frequency quadrupled Nd:YAG laser (266 nm) and a KrF<sup>\*</sup>-excimer laser (248 nm) at various fluences and pulse numbers. The plots of ablation depth versus pulse number at a given fluence clearly reveal that incubation takes place. Ablation starts only after several pulses. The obtained ablation rates were plotted versus the fluence (Fig. 2).

Eq. (1) [18,19] was used to calculate the threshold fluence ( $F_0$ ) and the effective absorption coefficient ( $\alpha_{\text{eff}}$ ) with  $d(F)$  as the etch rate at a given fluence  $F$ .

$$d(F) = \frac{2.3}{\alpha_{\text{eff}}} \log \left( \frac{F}{F_0} \right) \quad (1)$$

The ablation threshold fluence and an effective absorption coefficient are compiled in Table 1.

The significant differences in the ablation thresholds for both irradiation wavelengths presumably originate from the different pulse lengths of both lasers. Since the photon energies are very similar, ablation may be ascribed to a single and/or a multi-photon absorption process. Decomposition can take place starting from the polymer or embedded impurities photochemically [20–22], where electronic excitation results in direct bond breaking and/or photothermally [18,23,24] due to vibrational relaxation of excited states. Photothermal ablation processes are often accompanied by the observation of Arrhenius tails [25], the dependence of the ablation rate and threshold on the laser pulse repetition rate [26] and pulse length [27,28]. The details of the ablation mechanisms are still under discussion and other researchers have concluded

Table 1  
Comparison of the effective absorption coefficients and the threshold fluences for 248 and 266 nm irradiation

	248 nm	266 nm
Photon energy (eV)	5	4.7
Pulse length, $\tau$ (ns)	25	6
$\alpha_{\text{in}}$ (cm <sup>-1</sup> )	2.4	1.9
$\alpha_{\text{eff}}$ (cm <sup>-1</sup> )	32700 ± 800	48900 ± 2800
$F_0$ (mJ cm <sup>-2</sup> )	940 ± 160	210 ± 60

that photothermal and photochemical reactions both contribute with ratios depending on the ablation conditions and polymer properties [29–31]. The observed behavior of PDMS, i.e. the lower threshold fluence ( $210 \text{ mJ cm}^{-2}$ ) for the shorter pulse length (6 ns) can be explained by both mechanisms [18,19]. The ablation rate can be described in both cases by Eq. (1).

The effective absorption coefficient is very different to the linear absorption coefficient of  $\approx 2 \text{ cm}^{-1}$ . The incubation behavior is therefore closely related to an increase of absorption during irradiation with the initial laser pulses. Incubation of polymers is often related to chemical modifications only a few micrometers below the surface without altering the bulk properties of the polymer [13,14,19,32–34]. In our experiments, incubation is mainly taking place by local chemical transformations, which are located up to several hundred micrometers below the polymer surface. These domains are clearly visible in our optical microscope (Fig. 3). They are distributed statistically over the irradiated area. As soon as the absorption is high enough or a certain amount of local chemical transformation occurred, ablation takes place. The local chemical transformation or the formation of defects and internal micro structuring at different depths was to our knowledge only reported for polymers [15–17] and inorganic materials [35–40] upon irradiation with femtosecond and picosecond lasers. One possible explanation for the local chemical transformations in PDMS are impurities, e.g. remaining from the synthesis (e.g. Pt), which are the “seeds” for these transformations.

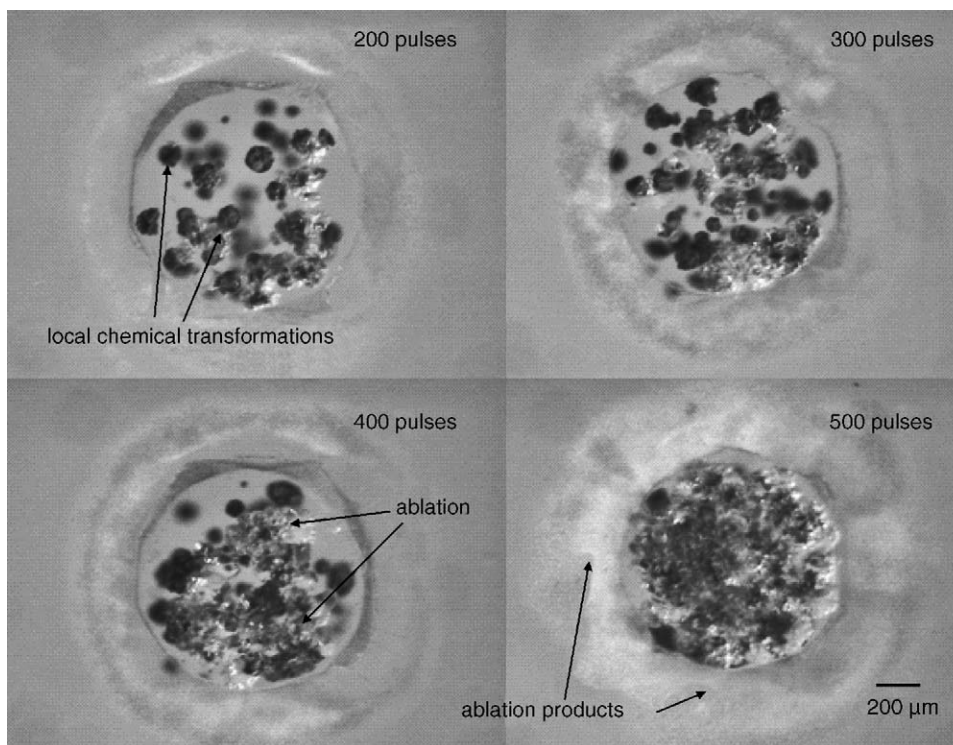


Fig. 3. Optical microscope photographs of irradiated PDMS samples (KrF<sup>\*</sup>-excimer laser, 248 nm,  $1 \text{ J cm}^{-2}$ , 200–500 pulses). The microscope was focused onto the surface. The local chemical transformations located below the surface appear less sharp. Areas of ablation and the ablation products are clearly visible.

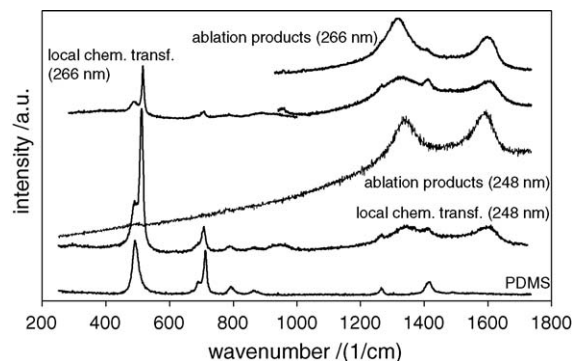


Fig. 4. Representative Raman spectra of native PDMS, the local chemical transformations and the ablation products after irradiation with the Nd:YAG (266 nm) and the KrF<sup>\*</sup>-excimer laser (248 nm).

### 3.2. Raman spectroscopy

The local chemical transformations have been studied by confocal Raman microscopy. Since PDMS is transparent in the visible, it is possible to record Raman spectra up to several hundred micrometers below the surface. The reference spectrum of the cross-linked PDMS is comparable to previous published data [41].

The Raman spectra of native PDMS differ significantly from the Raman spectra of the local chemical transformations after irradiation (Fig. 4). The Raman spectra of these domains are characterized by two distinct bands appearing around  $1330$  and  $1600 \text{ cm}^{-1}$ , a sharp band around  $510 \text{ cm}^{-1}$  and a

very weak band around  $940\text{ cm}^{-1}$ . The first two bands are very similar to those observed for polycrystalline graphite, amorphous carbon and a wide range of carbon fibers [42–44]. They correspond to the D- and G-bands of amorphous carbon, respectively [44]. The position, relative intensity, and bandwidth are related to crystalline domains in the carbon. A sharp and intense G-band and a small D-band indicate the presence of highly ordered pyrolytic graphite. Broader bands, which have an overlap and smaller intensities indicate more disordered structures [45]. Cho et al. [46] reported a broad weak band at about  $1400\text{--}1500\text{ cm}^{-1}$  appearing in the Raman spectra of amorphous carbon films.

In our experiments, the positions of the G-bands are very similar for both irradiation wavelengths ( $\sim 1597\text{ cm}^{-1}$  at  $248\text{ nm}$  and  $\sim 1603\text{ cm}^{-1}$  at  $266\text{ nm}$ ), suggesting that the graphitic structures in the local chemical transformations are very similar. At the same time the D-band position changes significantly. The D-band is located at  $\sim 1346\text{ cm}^{-1}$  after irradiation with the excimer laser ( $248\text{ nm}$ ) and at  $\sim 1320\text{ cm}^{-1}$  after irradiation with the Nd:YAG laser ( $266\text{ nm}$ ). The irradiation with shorter pulse length of the Nd:YAG laser for similar photon energies results in more disordered structures in the generated carbon, which is associated with the D-band position at lower wavenumbers. The same energy deposit within a shorter time frame causes more disorder in the created carbon.

The Raman band between  $502$  and  $520\text{ cm}^{-1}$  is detected in the spectra after irradiation with both lasers. The sharp vibration band is ascribed to mono- and/or polycrystalline silicon or only monocrystalline silicon [47].

The weak Raman band between  $906$  and  $960\text{ cm}^{-1}$  could only be detected in some cases, probably due to the low intensity and signal to noise ratio. Hobert et al. [48] described also a weak band at  $944\text{ cm}^{-1}$  and another weak band at  $790\text{ cm}^{-1}$  and attributed them to the LO and TO phonons of microcrystalline SiC [49]. The band at  $790\text{ cm}^{-1}$  cannot be assigned in our spectra because this overlaps with a band of native PDMS.

The Raman spectra of the ablation products which are deposited in the surrounding of the ablation crater exhibit the same characteristics as in the areas of chemical transformation. The D- and G-bands are located around  $1340$  and  $1588\text{ cm}^{-1}$  after irradiation with the KrF<sup>\*</sup>-excimer laser and around  $1330$  and  $1605\text{ cm}^{-1}$  after irradiation with the Nd:YAG laser [50]. This indicated that the carbon in the domains of chemical transformation are ejected during ablation without complete decomposition. In some spectra the mono- and polycrystalline silicon Raman band around  $510\text{ cm}^{-1}$  and the weak microcrystalline SiC band around  $940\text{ cm}^{-1}$  appear also.

### 3.3. Infrared spectroscopy

Infrared spectroscopy is another useful method for the investigation of changes in the chemical structure of polymers. Since the local chemical transformations below the polymer surface cannot be analyzed by this method we are limited to the analysis of the ablation products that are deposited on the surface. The ablation products of PDMS samples after irradiation with the KrF<sup>\*</sup>-excimer laser were studied

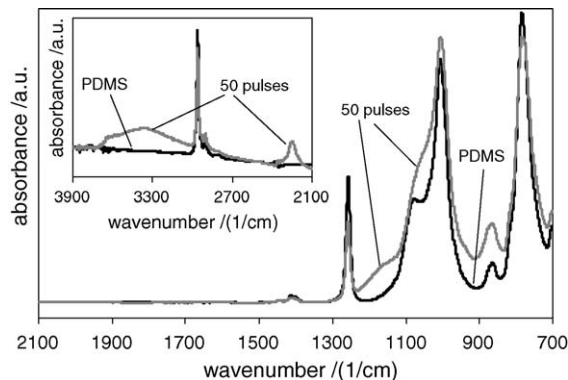


Fig. 5. ATR-FTIR spectra of native PDMS and the ablation products after irradiation with the KrF<sup>\*</sup>-excimer laser ( $248\text{ nm}$ ,  $4.8\text{ J cm}^{-2}$ , 50 pulses).

qualitatively by ATR-FTIR spectroscopy. The IR reference spectrum of the cross-linked PDMS is in accordance with previous published data [51].

The IR spectra of the ablation products show the absorption bands of the native PDMS and bands, which can be ascribed to ablation products (Fig. 5). This suggests that either the coverage of the PDMS with the ablation products is incomplete or that the layer is thin, i.e. below  $1\text{--}5\text{ }\mu\text{m}$ , which is the typical analytical depth of ATR-FTIR. The latter is of course very probable as layers of redeposited ablation products are typically in the nanometer range [52].

The spectra of the ablation products exhibit an OH absorption band centered between  $3300$  and  $3400\text{ cm}^{-1}$ . Besides intensity shifts of the Si–O absorption bands between  $900$  and  $1200\text{ cm}^{-1}$  the formation of a shoulder at  $1150\text{ cm}^{-1}$  has been observed. This suggests the formation of a new silicon oxide species. Lucovsky et al. [53] and Pai et al. [54] have calculated the infrared spectrum of SiO<sub>2</sub> and suggested that a broad shoulder at about  $1150\text{ cm}^{-1}$  is due to asymmetric stretching vibrations of oxygen atoms in a Si(O<sub>4</sub>) configuration.

Additionally an absorption band with very low intensity can be found at about  $2250\text{ cm}^{-1}$ . Lucovsky et al. [55] attributed a band between  $2246$  and  $2257\text{ cm}^{-1}$  to the stretching vibrations of Si–H groups. Its position depends on the number of oxygen atoms at the silicon as well as on the stoichiometry of the surrounding matrix. A comparison of the spectra of the ablation products with the experiments of Lucovsky et al. suggests a ratio of oxygen to silicon of 1.5.

The combination of the Raman and FTIR data suggests that the incubation products carbon, SiC or Silicon are deposited on the surface together with larger decomposition products of the polymer, which include silicon oxides and fragments with SiH and SiOH groups.

## 4. Summary

After irradiation of PDMS at  $266$  and  $248\text{ nm}$  and analysis of the ablation depth versus pulse number, a pronounced incubation behavior was observed. The thresholds of ablation and the corresponding effective absorption coefficients are determined. The significant differences in the ablation

thresholds for both irradiation wavelengths are probably due to the different pulse lengths of both lasers. Since the shorter pulse length is correlated with a lower ablation threshold incubation might originate from impurities in the polymer.

Normally incubation of polymers is related to changes of the chemical structure of the polymer. In our experiments, incubation is taking place by local chemical transformations up to several hundred micrometers below the polymer surface. These chemical transformations were studied by confocal Raman microscopy, and consist of carbon in the form of amorphous carbon with some crystalline features, mono- and/or polycrystalline silicon, and microcrystalline SiC.

The ablation products detected in the surroundings of the ablation crater consist mainly of carbon with some crystalline features, amorphous SiO<sub>x</sub> ( $x \approx 1.5$ ), low amounts of mono- and/or polycrystalline silicon, microcrystalline SiC and degraded polymer with SiH and SiOH groups.

### Acknowledgements

Financial support of the Bundesministerium für Bildung und Forschung (BMBF), the Swiss National Science Foundation and the EU Marie-Curie Training Site Fellowship is gratefully acknowledged.

### References

- [1] M. Brinkmann, V.Z.H. Chan, E.L. Thomas, V.Y. Lee, R.D. Miller, N. Hadjichristidis, A. Avgeropoulos, *Chem. Mater.* 13 (2001) 967.
- [2] V.N. Vasilets, T.I. Yuranova, A.N. Ponomarev, *J. Photopolym. Sci. Technol.* 7 (1994) 309.
- [3] V.N. Vasilets, K. Nakamura, Y. Uyama, S. Ogata, Y. Ikada, *Polymer* 39 (1998) 2875.
- [4] T.S. Phely-Bobin, R.J. Muisener, J.T. Koberstein, F. Papadimitrakopoulos, *Adv. Mater.* 12 (2000) 1257.
- [5] V.M. Graubner, R. Jordan, O. Nuyken, B. Schnyder, T. Lippert, R. Kotz, A. Wokaun, *Macromolecules* 37 (2004) 5936.
- [6] J. Kim, M.K. Chaudhury, M.J. Owen, *J. Colloid Interface Sci.* 226 (2000) 231.
- [7] H. Kim, M.W. Urban, *Langmuir* 15 (1999) 3499.
- [8] D.J. Wilson, R.C. Pond, R.L. Williams, *Interface Sci.* 8 (2000) 389.
- [9] G. Bar, L. Delineau, A. Hafele, M.H. Whangbo, *Polymer* 42 (2001) 3627.
- [10] H. Kim, M.W. Urban, *Langmuir* 12 (1996) 1047.
- [11] H. Hillborg, J.F. Ankner, U.W. Gedde, G.D. Smith, H.K. Yasuda, K. Wikstrom, *Polymer* 41 (2000) 6851.
- [12] H. Hillborg, U.W. Gedde, *Polymer* 39 (1998) 1991.
- [13] R. Srinivasan, B. Braren, K.G. Casey, *J. Appl. Phys.* 68 (1990) 1842.
- [14] S. Küper, M. Stuke, *Appl. Phys. A* 49 (1989) 211.
- [15] G. Zhou, M.J. Ventura, M.R. Vanner, M. Gu, *Appl. Phys. Lett.* 86 (2005) 011108.
- [16] K. Yamasaki, S. Juodkazis, M. Watanabe, H.B. Sun, S. Matsuo, H. Misawa, *Appl. Phys. Lett.* 76 (2000) 1000.
- [17] D. Day, M. Gu, *Appl. Phys. Lett.* 80 (2002) 2404.
- [18] S.R. Cain, F.C. Burns, C.E. Otis, *J. Appl. Phys.* 71 (1992) 4107.
- [19] S.R. Cain, F.C. Burns, C.E. Otis, B. Braren, *J. Appl. Phys.* 72 (1992) 5172.
- [20] E. Sutcliffe, R. Srinivasan, *J. Appl. Phys.* 60 (1986) 3315.
- [21] S. Lazare, V. Granier, *Laser Chem.* 10 (1989) 25.
- [22] G.D. Mahan, H.S. Cole, Y.S. Liu, H.R. Philipp, *Appl. Phys. Lett.* 53 (1988) 2377.
- [23] N. Bityurin, N. Arnold, B. Luk'yanchuk, D. Bäuerle, *Appl. Surf. Sci.* 127–129 (1998) 164.
- [24] N. Arnold, B. Luk'yanchuk, N. Bityurin, *Appl. Surf. Sci.* 127–129 (1998) 184.
- [25] S. Kueper, J. Brannon, K. Brannon, *Appl. Phys. A* 56 (1993) 43.
- [26] F.C. Burns, S.R. Cain, *J. Phys. D: Appl. Phys.* 29 (1996) 1349.
- [27] K. Piglmayer, E. Arenholz, C. Ortwein, N. Arnold, D. Bäuerle, *Appl. Phys. Lett.* 73 (1998) 847.
- [28] B. Luk'yanchuk, N. Bityurin, M. Himmelbauer, N. Arnold, *Nucl. Instrum. Methods Phys. Res. Sect. B* 122 (1997) 347.
- [29] T. Lippert, J. Stebani, J. Ihlemann, O. Nuyken, A. Wokaun, *J. Appl. Phys.* 97 (1993) 12296.
- [30] V. Srinivasan, M.A. Smrtic, S.V. Babu, *J. Appl. Phys.* 59 (1986) 3861.
- [31] A.D. Zweig, V. Venugopalan, T.F. Deutsch, *J. Appl. Phys.* 74 (1991) 4181.
- [32] G.B. Blanchet, P. Cotts, C.R. Fincher Jr., *J. Appl. Phys.* 88 (2000) 2975.
- [33] S.I. Bozhevolnyi, I.V. Potemkin, *J. Phys. D: Appl. Phys.* 27 (1994) 19.
- [34] D.J. Krajnovich, *J. Phys. Chem. A* 101 (1997) 2033.
- [35] A. Rosenfeld, M. Lorenz, R. Stoian, D. Ashkenasi, *Appl. Phys. A* 86 (1999) S373.
- [36] D. Ashkenasi, M. Lorenz, R. Stoian, A. Rosenfeld, *Appl. Surf. Sci.* 150 (1999) 101.
- [37] Y. Dong, P. Molian, *Appl. Phys. A* 77 (2003) 839.
- [38] M.H. Hong, B. Lukyanchuk, S.M. Huang, T.S. Ong, L.H. Van, T.C. Chong, *Appl. Phys. A* 79 (2004) 791.
- [39] E.N. Glezer, E. Mazur, *Appl. Phys. Lett.* 71 (1997) 882.
- [40] S. Juodkazis, K. Yamasaki, A. Marcinkevicius, V. Mizeikis, S. Matsuo, H. Misawa, T. Lippert, *Mater. Res. Soc. Symp. Proc.* 687 (2002) 173.
- [41] L. Jayes, A.P. Hard, C. Sene, S.F. Parker, U.A. Jayasooriya, *Anal. Chem.* 75 (2003) 742.
- [42] P. Lespade, R. Al-Jishi, M.S. Dresselhaus, *Carbon* 20 (1982) 427.
- [43] D.S. Knight, W.B. White, *J. Mater. Res.* 4 (1989) 385.
- [44] F. Tuinstra, J.L. Koenig, *J. Chem. Phys.* 53 (1970) 1126.
- [45] J. Robertson, *Adv. Phys.* 35 (1986) 317.
- [46] N.-H. Cho, K.M. Krishnan, D.K. Veirs, M.D. Rubin, C.B. Hopper, B. Bhushan, D.B. Bogy, *J. Mater. Res.* 5 (1990) 2543.
- [47] C. Palma, M.C. Rossi, C. Sapia, E. Bemporad, *Appl. Surf. Sci.* 138–139 (1999) 24.
- [48] H. Hobert, H.H. Dunken, S. Urban, F. Falk, H. Stafast, *Vib. Spectrosc.* 29 (2002) 177.
- [49] Y. Ward, R.J. Young, R.A. Shatwell, *J. Mater. Sci.* 36 (2001) 55.
- [50] V.-M. Graubner, R. Jordan, O. Nuyken, T. Lippert, M. Hauer, B. Schnyder, A. Wokaun, *Appl. Surf. Sci.* 197–198 (2002) 786.
- [51] J. Morvan, M. Camelot, P. Zecchini, C. Roques-Carmes, *J. Colloid Interface Sci.* 97 (1984) 149.
- [52] F. Raimondi, S. Abolhassani, R. Brutsch, F. Geiger, T. Lippert, J. Wambach, J. Wei, A. Wokaun, *J. Appl. Phys.* 88 (2000) 3659.
- [53] G. Lucovsky, C.K. Wong, W.B. Pollard, *J. Non-Cryst. Solids* 59–60 (1983) 839.
- [54] P.G. Pai, S.S. Chao, Y. Takagi, G. Lucovsky, *J. Vac. Sci. Technol. A* 4 (1986) 689.
- [55] G. Lucovsky, J. Yang, S.S. Chao, J.E. Tyler, W. Czubytyj, *Phys. Rev. B: Condens. Matter* 28 (1983) 3225.